IEEE Access
Multidisciplinary ⁝ Rapid Review ⁝ Open Access Journal

Received December 11, 2018, accepted January 27, 2019, date of publication February 13, 2019, date of current version March 1, 2019.

*Digital Object Identifier 10.1109/ACCESS.2019.2899080*

# Detection of Peat Fire Risk Area Based on Impedance Model and DInSAR Approaches Using ALOS-2 PALSAR-2 Data

**JOKO WIDODO[1,2], (Member, IEEE), YUTA IZUMI[3], (Student Member, IEEE), AYAKA TAKAHASHI[1], HUSNUL KAUSARIAN[4], DANIELE PERISSIN[5], (Member, IEEE), AND JOSAPHAT TETUKO SRI SUMANTYO[1], (Senior Member, IEEE)**

[1]Center for Environmental Remote Sensing, Chiba University, Chiba 263-8522, Japan
[2]Agency for the Assessment and Application of Technology, South Tangerang 10340, Indonesia
[3]Graduate School of Environmental Studies, Tohoku University, Sendai 980-8576, Japan
[4]Geological Engineering Department, Universitas Islam Riau, Pekanbaru 28284, Indonesia
[5]Lyle School of Civil Engineering, Purdue University, West Lafayette, IN 47907, USA

Corresponding author: Joko Widodo (joko.widodo@bppt.go.id)

This work was supported in part by the 4th Japan Aerospace Exploration Agency (JAXA) ALOS Research Announcement under Grant 1024, in part by the 6th JAXA ALOS Research Announcement under Grant 3170, in part by the Japanese Government National Budget–Ministry of Education and Technology (MEXT) FY2015–2017 under Grant 2101, in part by the Chiba University Strategic Priority Research Promotion Program under Grant FY2016-FY2018, in part by the Ministry of Research, Technology and Higher Education Republic of Indonesia through the Program Research and Innovation in Science and Technology (RISET-Pro) World Bank Loan under Grant 8245-I, in part by the Siak Regency Local Government, Riau Province, Indonesia, in part by the Universitas Islam Riau (UIR), Indonesia, and in part by the Josaphat Microwave Remote Sensing Laboratory (JMRSL), Chiba University.

**ABSTRACT** Forest fire in Indonesia occurs mostly in peatland area. Dry peatland areas with groundwater table (GWT) more than 40 cm from the soil surface have become degradation areas with high potentials to fire. This paper presents a new novel to detect a peat fire risk area by incorporating two methods: the impedance model and the differential interferometric SAR (DInSAR) technique which is based on the knowledge of annual subsidence rate associated with the GWT. The previous impedance model is modified in this paper by integrating the surface roughness information in the model as a part of novelty. The proposed method was then validated with ground truth data of GWT. By using an impedance model, this paper successfully detected peat fire risk area based on the backscattering coefficient simulation of dry peatland. Based on the simulation model, the average, minimum, and maximum of backscattering coefficient of dry peat are −13.97, −11.5, and −17.29 dB, respectively. The correlation coefficient between the simulated backscattering coefficient and backscattering from ALOS-2/PALSAR-2 data is 0.8 with root mean square error of 1.4. By using the DInSAR method, detection of dry peatland area was successful. The significant relationships confirmed between GWT measurement and model are 0.71 for Pair A and 0.85 for Pair B. Both methods showed that peat fire risk areas were identified successfully. The dielectric constant of the peat soil also revealed that the soil condition of the area of interest is very dry indicating the potential to peat fire risk. Employing two models, respectively, were recommended to get precision of detection analysis.

**INDEX TERMS** Detection of peat fire risk area, impedance model, DInSAR, ALOS-2 PALSAR-2 data.

## I. INTRODUCTION

Indonesia has the largest peatland area in Southeast Asia (47%), besides Malaysia (6%), Papua New Guinea (3%), and smaller area amounting 1% spreading in Brunei, Myanmar, Thailand, and Vietnam. Conservation and rehabilitation of peat-forest area in Indonesia have been conducted however it remains the largest area because of (1) human impact such as plantations of oil palms, rubber, pulp trees, and food production, and (2) the great impact of climate changes including El Nino, La Nina, and ENSO [1].

Forest fire is the main problem in Indonesia starting in 1982 when 75% of the forest fire is occurred in peatland area, mainly in open area [2]. Between 1990 and 2015, almost 27.5 million ha of forest had changed into logging, fires, timber, pulpwood, and palm oil plantations, and now of the 75%,

The associate editor coordinating the review of this manuscript and approving it for publication was Weimin Huang.

only 50% area remains covered in the forest. The worst of forest fires take placed in 1997/1998 and 2006 during El Nino with 140.000 hotspots. The similar condition occurred in 2015 when forest fire started at the end of June 2015 and could only be stopped after the start of the rainy season in November 2015 [3], [4].

During June and October 2015, 2.6 million hectare of Indonesia land burned and equal to four and half time the size of Bali Island. More than 100,000 of hostpots area is man-made fires were used to prepare land for agriculture and to gain access to land cheaply. Eight provinces; South Sumatera, Central Kalimantan, South Kalimantan, West Kalimantan, East Kalimantan, Riau, Jambi, and Papua had burned more than 100,000 hectares. Sumatera and Kalimantan Island are the hardest hit by fire were most of the peatland are located [3] with total burned area 23% for Sumatera and 16% for Kalimantan. Papua also contributed 10% area burnerd of the total area burned nationality, even though, peatland in Papua are some of the last intact in Indonesia [3].

In 2015, the fire destroyed rainforest that was a home of wildlife such as the Asian elephant (Elephas maximus), tiger (Panthera tigris), rhinoceros (Dicerorhinus sumatrensis harrissoni) and orang-utans (Pongo spec.). The fire and smoke affected the habitats of Orang Utan in Kalimantan and elephant and tiger in SumatraIndonesia ranks fifth as the top level of Green House Gas emitters after China, USA, India, and Russia; nevertheless, after a forest fire in 2015, Indonesia became the fourth largest emitters. From 2000 to 2005, Indonesia's annual emissions from forest and peat soil oxidation was around 800 million t $CO_2$ which is almost the same as Germany‘s annual emissions. If compared to emissions from Riau Province in Sumatera, the emissions from Sumatera alone are around 3.66 billion t $CO_2$ that is released into the atmosphere, 1.39 billion t of which was released by burning peat soils, and the other 0.78 billion t $CO_2$ by decomposition processes in drained peat soils [3].

Forest fire and fire smog in Indonesia has caused considerable economic losses to the country, around 200 million US$ in the period of 1997 – 2007 [4], and in 2015, the losses were at least 16.1 billion US$ or equivalent with 1.9% of GDP [5]. This forest fire and fire smog also affected to the neighboring countries such as Malaysia, Singapore, Thailand, and Brunei [3].

Indonesia needs participation from international prevention project and community because prevention is the most important aspect of a successful fire management system. Regular monitoring and data collection should be conducted and an early warning system on the province level is equally necessary [4]. Therefore, The Canadian Forest Fire Danger Rating System (FDRS) was installed in Indonesia starting from 2004 based on weather information: temperature, relative humidity, wind speed, and rainfall. The result is the Fire Weather Index (FWI) [5].

By using optical remote sensing data such as MODIS satellite data has shown its capability to detect a variety of large scales of the pattern of fuel connectivity which can be used for monitoring pattern of fire danger with graph theory [6]. Remote sensing plays the main role in the development of fuel maps in order to assess live fuel moisture among the most basic of the fire environment: topography, fuels, and weather [7]. NOAA-AVHRR is confirmed as option input data too, especially in soil moisture detection and understanding as an indicator of fire danger [8]. The main problems in optic satellite data are the fact that the soil surface information is not available under the cloudy condition and night condition. Synthetic Aperture Radar (SAR) on the other hand provides surface information with the advantage by the capability to penetrate clouds cover, penetrate rain in some intensity, and also can be operating in the nighttime. These all capabilities are important to complement the optical disability [9] and give strong reason to employed SAR data in this research.

The study by using SAR data [10] shown that there is a strong relationship between backscattering coefficient and FWI by means of Canadian C-band SAR of RADARSAT-1. Other studies evaluated ERS SAR sensor for prediction of fire danger in a boreal region, where the correlation between burn backscatter, forest backscatter, and FWI is also significant [11]. The study [12] reveals method in order to monitor spatial and temporal surface soil moisture in fire that disturbed boreal forest, and also [13] for live fuel moisture monitoring in semi-arid area. Recently, our research group also has developed novel soil moisture retrieval by using SAR data, which is of importance for peat fire risk monitoring [14].

PALSAR and PALSAR-2 are popular sensors of SAR L-Band Frequency as a part of Advanced Land Observation (ALOS) Satellite with ownership by Japan Exploration Space Agency (JAXA). These sensors have possibility as an input data to monitor various conditions in peatland area such as forest biomass change, soil moisture, water level, peat dome detection, peat thickness, and peat subsidence [15], and groundwater table [16].

In the peatland area, there is a relationship between the groundwater table and fire occurrence. When the groundwater table is deeper, peatland is easier to burn. Therefore, the groundwater table can be a good indicator for peat fire risk zone mapping at peatland area [17]. Regulation in Indonesia mentions that peatland with groundwater table more than 40 cm is included to the degradation peatland area [18], [19] and has high potential to fire.

By using impedance model that considers the relationship between dielectric constant, incident angle and backscattering coefficient, ALOS data is also effective to detect soil moisture [20] burn coal seam thickness [21] thickness of fire scars [22], topsoil thickness [23], and layer thickness estimation of silica sand distribution [24]. However, the impedance model is developed by assuming no surface roughness, contrary to the actual conditions in the field.

A few studies have shown the applicability of DInSAR technique to detect the peatland degradation area. Basically, DInSAR extract the phase differences between two SAR images and convert to the deformation (subsidence) information after removed the topography contribution to the interferogram using a Digital Elevation Model (DEM) [25], [26]. Many studies used subsidence information as indicator of degraded peatland and as input parameter to retrieve the groundwater table and others in the peatland area [26]–[29].

This research employed new impedance model and DInSAR approach to detect peatland fire risk areas. In this new impedance model, soil roughness parameter is considered as a new parameter of circuit model and as an independent layer to enrich an impedance model based on transmission line theory. This is an innovation of this research compared to others [20]–[24]. The combination of methods with DInSAR will provide more precise analysis results by utilizing phase information from image SAR. This combination method also innovation of this research in order to detect peat fire risk area compare with other studies previously [6]–[13]. The addition of soil roughness parameters to the model impedance and its combination with DInSAR provide advantages in the form of accuracy of the analysis and for mutual cross check.

## II. BACKGROUND OF STUDY AREA

The study area was located in Sungai Apit, Siak Regency, Riau Province, Indonesia. It is about 37 km away from the downtown of Siak City.

### A. LOCATION AND CLIMATE

Siak Regency is from latitude 1°16'30" until 0°20'49" and longitude 100°54'21" to 102°14'50" in Riau Province, Sumatera. The study area is the eastern part of Siak Regency [30]. Siak has weather temperature between $25^0$ and $32^0$ Celsius as the area under tropical climate condition.

### B. GEOLOGY

The peat is the youngest deposits in central Sumatera which are dominantly metaquartzite, granite, and tuff. Almost 51% geologic structures in Riau mostly consist of peat deposits, and 93% of deposit is ombrogenous peat swamp forest. In the study area, the topographic indicated that the peat deposits type is peat domes with the maximum peat thickness is about 13 m [31]

### C. LAND USE

Land use of this area is mostly plantation or agriculture area where plantation is managed by the company or private. Fig. 1 shows that there are some types of peatland surrounding area; peatland dome with canal and peatland dome without canals. Some areas were also affected by fire in 2015. During the field survey, forest fire also occurred in some part area.

## III. MATERIALS AND METHODS

### A. MATERIALS

#### 1) SATELLITE DATA

This research used the scene of SAR satellite data ALOS-2 PALSAR 2 provided by JAXA. Four images of ALOS-2 data were on August 30, 2014, May 9, 2015, March 25, 2017, and August 2, 2017 to be processed in this research.

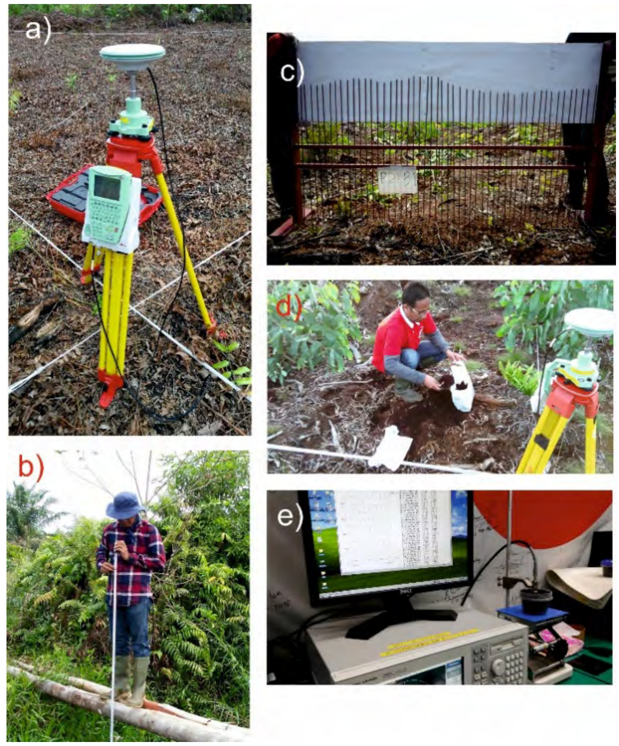


**FIGURE 1.** (a) Position measurement using DGPS, (b) Groundwater level Measurement, (c) Soil roughness measurement, (d) Soil sampling, (e) Soil dielectric constant measurement.

**TABLE 1.** Ground survey and sampling positions.

| Point No. | Position | |
|---|---|---|
| | Latitude | Longitude |
| 1 | 0.83492 | 102.37277 |
| 2 | 0.83273 | 102.37481 |
| 3 | 0.82263 | 102.37227 |
| 4 | 0.82965 | 102.37302 |
| 5 | 0.82721 | 102.37461 |
| 6 | 0.85234 | 102.35321 |
| 7 | 0.81651 | 102.35446 |
| 8 | 0.81551 | 102.35495 |
| 9 | 0.81636 | 102.35321 |
| 10 | 0.81511 | 102.35376 |
| 11 | 0.81576 | 102.35406 |
| 12 | 0.81183 | 102.35207 |
| 13 | 0.84194 | 102.35983 |
| 14 | 0.84274 | 102.36142 |
| 15 | 0.84751 | 102.35978 |
| 16 | 0.84846 | 102.36789 |
| 17 | 0.84592 | 102.37207 |
| 18 | 0.84527 | 102.37232 |

#### 2) GROUND SURVEY AND SAMPLING

Field survey and samples were collected from July 26 to August 10, 2017. The soil sampling was conducted in the peatland area, consisting of 18 samples points. Positions were measured by handheld GPS, and some point verification by DGPS (Leica 1200 +). Soil samples were then brought to laboratory to measure real and imaginary part of

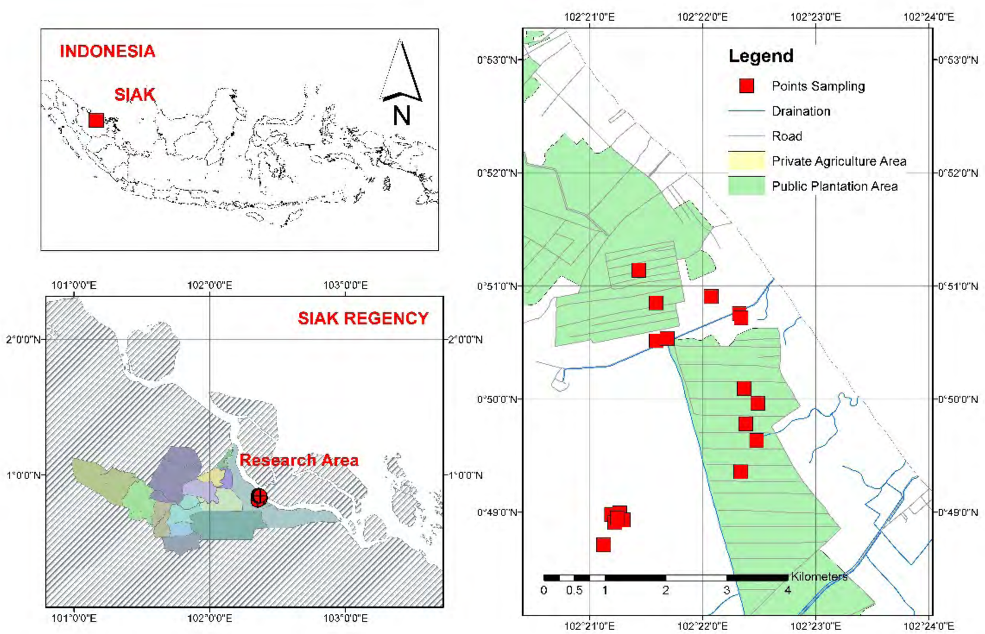


**FIGURE 2. Research Location in Sungai Apit, Siak Regency, Riau Province, Sumatera Island, Indonesia. Point red color is research position area consist of 18 points. The coordinate position of points sampling shown in Table. 1.**

dielectric constant by dielectric constant probe kit (Agilent model 85070E) with a network analyzer (VNA). In order to measure surface roughness, soil surface roughness meter consisting of 25 needles was used. Field survey activities of this research are shown in Fig 1, where research location and the points sampling shown in Fig.2

### *B. METHODS*

Basically, in this research, there are two methods proposed to detect peatland risk area. First, an impedance model was used to compare backscattering coefficient between SAR data and simulated backscattering coefficient of the dry peat soil of the surface area. The second method was DInSAR that was used to extract the groundwater table information based on the displacement (subsidence) rate condition. Flowchart diagram involved in this method is shown in Fig.3.

#### 1) IMPEDANCE MODEL APPROACH

An impedance-based approach using the concept of the transmission line theory was used in this research. Impedance model is developed based on the concept of transmission line theory by which series impedance of surface roughness, peatland, and soil layer. Scattering mechanism of the model is shown in Fig. 5 while circuit model is shown in Fig.4. Based on the scattering mechanism, the model consists of 4 layers: the air layer, soil roughness layer, peatland layer, and a soil layer.

For the model, it is assumed that media is composed of an infinite length of air, surface roughness, peatland and soil layer of thickness t. Impedance-based model is represented by the three-dimensional model.

Based on the circuit model,*ZR* represents effective series of impedance soil roughness layer, *ZP* and *ZS* represent the parallel model of peatland layer, and *ZP* represents total input impedance. In this research, the complexity of the analysis was reduced by negligible parallel impedance of soil layer (*ZS*) and hence considered as zero. The limitations of the penetration of electromagnetic waves in deep soil are the reason.

The incident wave *E0* is also considered to be a plane wave with incident angle $\theta$i [20] then the total input impedance model for surface roughness is determined by:

$$ZT1 = ZR\frac{Z_P + ZR\tanh\gamma c^t}{Z_R + ZP\tanh\gamma c^t} \tag{1}$$

The model above is parallel with total input impedance model for peatland layer that is determined by:

$$ZT2 = ZP\frac{Z_S + ZP\tanh\gamma c^t}{Z_P + ZS\tanh\gamma c^t} \tag{2}$$

Based on the equation above, $\gamma$C is the propagation constant of the surface roughness and peatland layer. Snell law is also applied at the boundary between air, surface roughness and peatland layer, and expressed by the following relationship,

$$\sin\theta_i = \sqrt{\varepsilon_r\mu_1}\sin\theta_1 \tag{3}$$

where $\theta i$ is transmission angle, $\varepsilon_r$, $\mu_r$, are complex dielectric constant, and complex specific permeability of surface roughness and peatland layer, then the propagation constant is obtained as,

$$\boldsymbol{\gamma_c = j\frac{2\pi}{\lambda}\sqrt{\varepsilon_r\mu_r - \sin^2\theta i}} \tag{4}$$

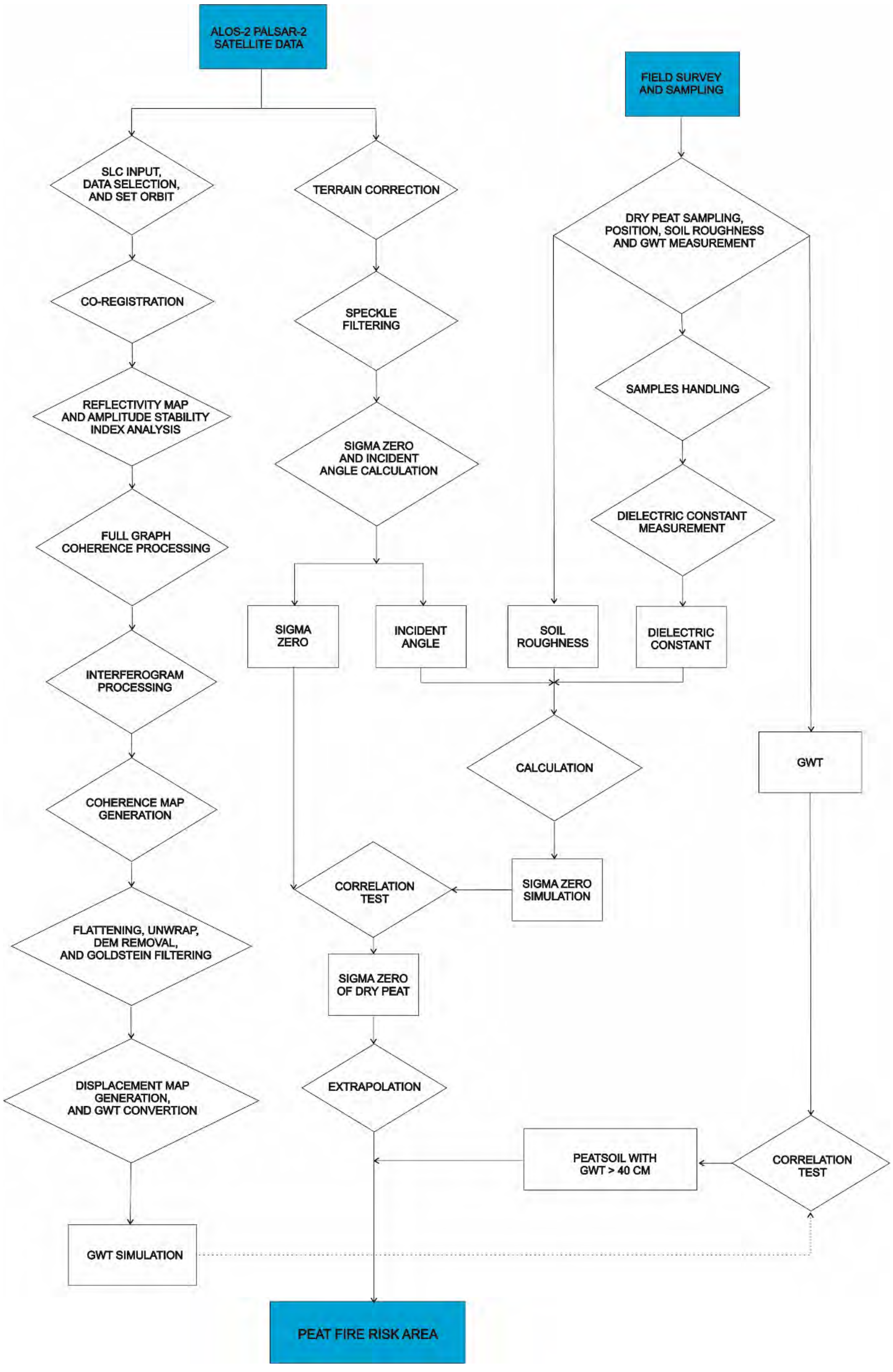


**FIGURE 3.** Flow chart of research.

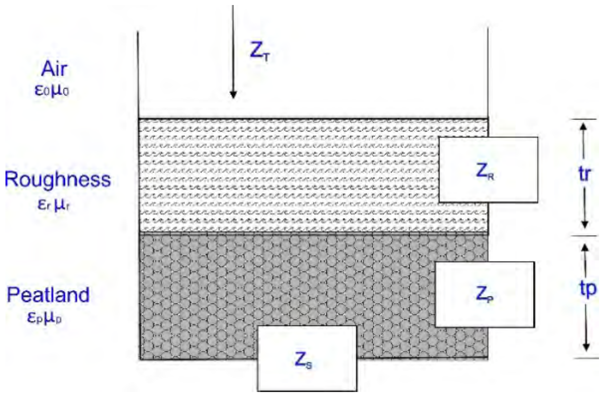


**FIGURE 4.** Circuit model approach used in this research. Surface roughness is proposed as a medium between air and peatland.

The effective of series impedance surface roughness layer ($\mathbf{Z_R}$),

$$\mathbf{Z_R = Z_0\sqrt{\frac{\varepsilon_r}{\mu_r}}\cos\theta_i}$$

and

$$Z_P = Z_R\sqrt{\frac{\varepsilon_r}{\mu_r}}\cos\theta_i \tag{5}$$

thus, the parallel impedance of peatland layer is express as,

$$\mathbf{Z_P = Z_R\sqrt{\frac{\varepsilon_r}{\mu_r}}\cos\theta_i} \tag{6}$$

The equation for the effective series impedance surface roughness layer can be represented as,

$$\mathbf{Z_{T1} = \frac{Z_0}{\varepsilon_r}\sqrt{\varepsilon_r\mu_r - \sin^2\theta_i} \times \tanh\left(j\frac{2\pi t}{\lambda}\sqrt{\varepsilon_r\mu_r - \sin^2\theta_i}\right)} \tag{7}$$

Parallel with an impedance of peatland layer that can be represented as:

$$\mathbf{Z_{T2} = \frac{Z_R}{\varepsilon_r}\sqrt{\varepsilon_r\mu_r - \sin^2\theta_i} \times \tanh\left(j\frac{2\pi t}{\lambda}\sqrt{\varepsilon_r\mu_r - \sin^2\theta_i}\right)} \tag{8}$$

Then $\mathbf{Z_T}$ is calculated as parallel circuit function by

$$\mathbf{Z_T = \frac{1}{Z_{T1}} + \frac{1}{Z_{T2}}} \tag{9}$$

Based on the equation above, the reflection of the coefficient is then calculated by

$$\mathbf{\Gamma = \frac{Z_T - Z_0\cos\theta_i}{Z_T + Z_0\cos\theta_i}} \tag{10}$$

Backscattering coefficient based on the impedance model then obtained

$$\sigma^0_{cal} = \mathbf{20}\log|\mathbf{\Gamma}| \tag{11}$$

The model above is a nonlinear function of complex dielectric constant and thickness of the surface roughness and peatland layer of the backscattering coefficient. The thickness of surface roughness is measured in the ground by using soil roughness meter. In order to simplify the model, in this research the thickness of peatland is considered same with λ for L-band frequency 23.5 cm.

### 2) DIFFERENTIAL INTERFEROMETRY SYNTHETIC APERTURE RADAR (DInSAR) APPROACH

This research used DInSAR approach based on interferogram that developed from a coherence technology of active radar imaging. Graham in 1974, first time carried out experience about DInSAR. Recently, DInSAR has developed and been

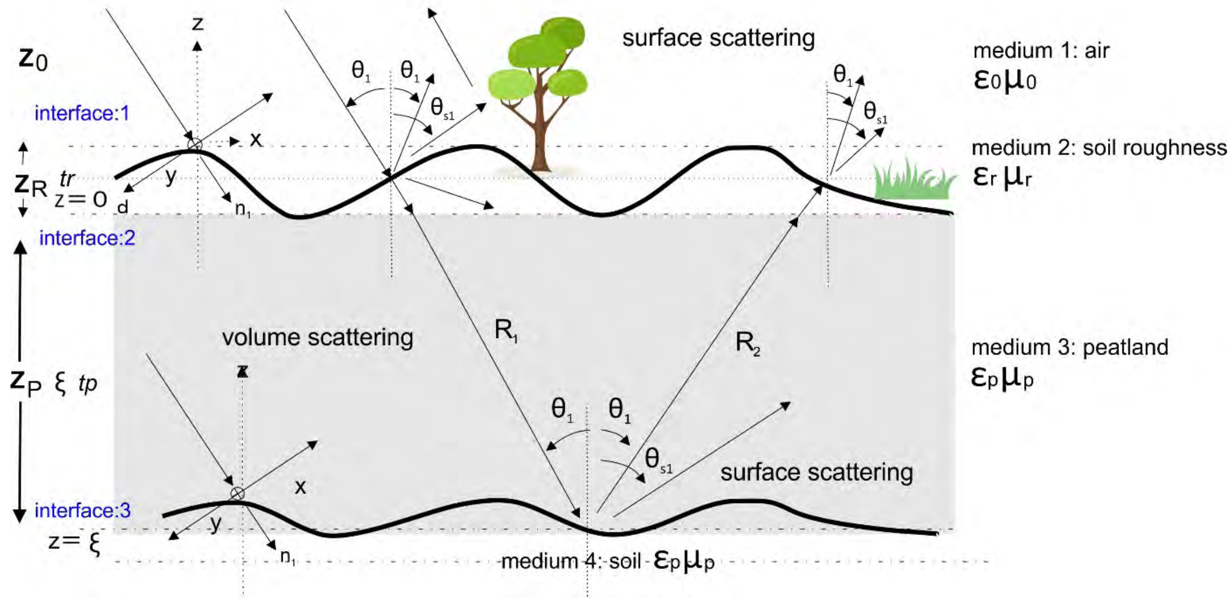


**FIGURE 5.** Impedance model approach used in this research. Surface roughness is proposed as a medium between air and peatland.

very useful to identify the phenomenon in the earth like subsidence and land movement including DInSAR coherence and subsidence in the peatland area [25].

Two images acquired with the same nominal geometry is required to develop interferometry SAR by using phase as a fraction of the wave and change to distance. The distance with sub-millimeter precision can develop since microwave signals have a wavelength in centimeter. One single image is used as a reference, and another image is used as a slave for resampled on the same sampling grade from the master image. The pixel coordinate in range call sample and pixel coordinate in azimuth call lines, so that image is called $Img_i(s,l)$ the complex value of image $i$ at coordinate $s,l$. and showing the corresponding phase value ø [25].

The phase value then can be expressed as a function of its distance $Ri$ from the sensor, an equation is

$$\o = \frac{4\pi}{\lambda} Ri \tag{12}$$

where ø is a phase, λ is wavelength, in this case, is the wavelength of L-band is 23.5 cm.

The interferogram between images $i$ and $k$ can be expressed as

$$Int_{ik}(s,l) = Img_i(s,l) .Img_k^*(s,l) \tag{13}$$

when the product is applied pixel by pixel and the star sign indicates the complexity of the conjugate, then the interferometric phase between images I and k can be expressed as

$$\o_{ik}(s,l) = \o_i(s,l) .\o_k(s,l) \tag{14}$$

and by combining 2 equations before, the equation can be expressed as

$$\o_{ik}(s,l) = \frac{4\pi}{\lambda}[R_i(s,l) - R_k(s,l)] \tag{15}$$

Normal baseline $B$n is the relative position between master and slave images in term of distance laterally the direction normal to the reference slant range, with a relationship with incidence angle $\Delta\theta$ as

$$\Delta\theta = \frac{Bn}{R_k} \tag{16}$$

where the master range of reference point O is $R_k = S_kO$ and the relative of interferometric is thus

$$\Delta\o_{ik} = \o_{ik}(P) - \o_{ik}(O) = \frac{4\pi}{\lambda}[R_{ik}(P) - R_{ik}(O)] \tag{17}$$

The relative interferometric phase can be expressed

$$\Delta\o_{ik} = \Delta\o_{ik}^{flat} + \Delta\o_{ik}^{height} \tag{18}$$

where respectively flat terrain and topographic (height) phase terms

$$\Delta\o_{ik}^{flat} = \frac{4\pi}{\lambda}\frac{Bn}{R_k}\frac{\Delta r}{\tan\theta} \quad \text{and} \quad \Delta\o_{ik}^{height} = \frac{4\pi}{\lambda}\frac{Bn}{R_k}\frac{\Delta h}{\sin\theta} \tag{19}$$

The flat terrain phase is then removed due to not carrying useful for any kind of applications; the process is called interferogram flattening. The ambiguity height is $\Delta h_a$, the height that generates a phase rotation is equal to 2λ, and then is calculated by

$$\Delta h_a = \frac{\lambda R_k sin\theta}{2B_n} \tag{20}$$

The next step is to remove the topographic phase then Differential Interferometric phase can be generated based on equation

$$\Delta\o_{ik}^{DInSAR} = \Delta\o_{ik} - \Delta\,\o_{ik}^{flat} - \Delta\,\o_{ik}^{height} \tag{21}$$

After this, Goldstein filtering 5 x 5 is employed and phase ambiguities are solved by using Unwrapping

$$\Delta\o_{ik}^{UW}(s,l) = \o_{ik}(s,l) \pm 2n\pi \tag{22}$$

Then, the groundwater table (GWT) is calculated based on Woosten Model [29]:

$$S = 0.04\,x\,GWT \tag{23}$$

where S is annual rates subsidence (cm/year) and GWT is groundwater table depth (cm) of the tropical peatland area.

#### 3) BACKSCATTERING COEFFICIENT CALCULATION

Backscattering coefficient (sigma naught/sigma zero) is calculated based on calibration method by JAXA for ALOS-2 PALSAR-2 data Level 1.1. (Single Look Complex)

$$\sigma^o = 10 * \log_{10} < DN^2 > -CF + A \tag{24}$$

where $\sigma^o$ is backscattering coefficient, and DN is digital number, CF is correction factor for Level 1.5 and Level 2.1 ALOS-2 data (−83 dB) and A is correction factor for Level 1.1. ALOS-2 data = 32 dB [32].

## IV. RESULT AND DISCUSSION

### A. RELATIONSHIP BETWEEN DIELECTRIC CONSTANT OF PEAT AREA AND GROUND WATER TABLE

In order to understand the relationship between dielectric constant and groundwater table, the correlation between the dielectric constant and groundwater table is calculated by Mc. Pearson correlation method and linear regression.

The result of dielectric constant both a real part and imaginary part measured is shown in the Table 2. below

Dielectric constant is the most important component related to an electromagnetic wave in term of backscattering scattering from the earth sent back to the satellite. Dielectric constant is influenced by soil moisture and soil texture. Dielectric constant will increase when soil moisture increases [33].

Forest fire in peatland area is mostly caused by dry peat condition. Dry peat condition in the dry season is influenced by groundwater table condition.

In this research, dielectric constant real parts of peat soil samples average in L-Band Frequency 1.275 GHz were 2.9,

**TABLE 2.** Dielectric constant (real and imaginary part), incidence angle and soil roughness measured of each points sample.

| Point No. | Dielectric Constant Real Part | Dielectric Constant Imaginary Part | Groundwater Table (cm) |
|---|---|---|---|
| 1 | 3.2219 | 0.19 | 84 |
| 2 | 3.8458 | 0.25 | 68 |
| 3 | 3.4452 | 0.26 | 65 |
| 4 | 2.7105 | 0.17 | 86 |
| 5 | 2.7379 | 0.33 | 87 |
| 6 | 2.1517 | 0.17 | 101 |
| 7 | 2.7166 | 0.19 | 88 |
| 8 | 2.7184 | 0.21 | 88 |
| 9 | 3.3677 | 0.19 | 88 |
| 10 | 3.0056 | 0.26 | 88 |
| 11 | 2.5591 | 0.21 | 88 |
| 12 | 3.7626 | 0.19 | 87 |
| 13 | 3.1726 | 0.24 | 81 |
| 14 | 2.8511 | 0.23 | 87 |
| 15 | 2.4919 | 0.21 | 82 |
| 16 | 2.0697 | 0.18 | 100 |
| 17 | 2.5162 | 0.29 | 102 |
| 18 | 2.87 | 0.24 | 102 |

minimum 2.07, and maximum 3.84. The average dielectric constant imaginary part of samples was 0.22, minimum 0.17, and maximum 0.33. This dielectric constant indicated the condition is very dry and has high-risk potential to fire.

Groundwater table is an important indicator in the term to detect peat fire risk area. Regulation in Indonesia mentions that peatland that has groundwater table more than 40 cm is under the degradation condition [18], [19]. Based on previously research, when groundwater table drops under 40 cm, soil moisture will decrease from 0.9 cm3/cm3 at saturation to about 0.50 $cm^3/cm^3$ at a pressure head of −4 kPa. This condition will lead to peat fire spreading quickly [34]–[39].

During this survey, the groundwater table was measured from the canals or holes near the point sampling. Average groundwater table conditions from 18 points sampling are 87.33 centimeters, minimum 65 centimeters, and a maximum 102 centimeters, as shown in Table.2

The correlation was then calculated to understand the relationship between dielectric constant and the groundwater table. By using linear regression, the correlation coefficient between the dielectric constant real part and groundwater table was 0.7 and coefficient determination ($R^2$) was 0.5. It means there is a significant relationship. The relationship between dielectric constant and groundwater table can be expressed

$$Y = -13.947x + 127.79 \tag{25}$$

where y is the groundwater table and x is a dielectric constant real part. The relationship graph between the dielectric constant real part and groundwater table is shown in Fig.6

The relationship and equation indicated that the smaller dielectric constant, the deeper the groundwater table and the drier the peat soil, the higher the potential to burn.

The relationship between the dielectric constant imaginary part and the groundwater table is very small, around 0.17.

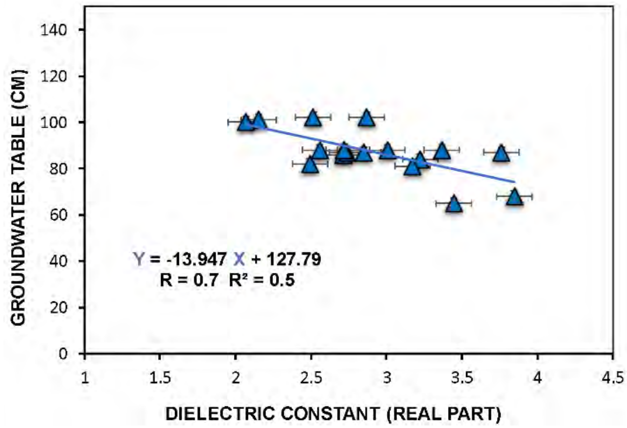


**FIGURE 6.** Relationship graph between dielectric constant (Real Part) and groundwater table condition. The relationship is significant with correlation coefficient (R) 0.7, and determinant coefficient ($R^2$) 0.5 Equation linear is $Y = -13.947X + 127.79$, where Y = groundwater Table (GWT) in centimeter unit (CM), and X = dielectric constant real part.

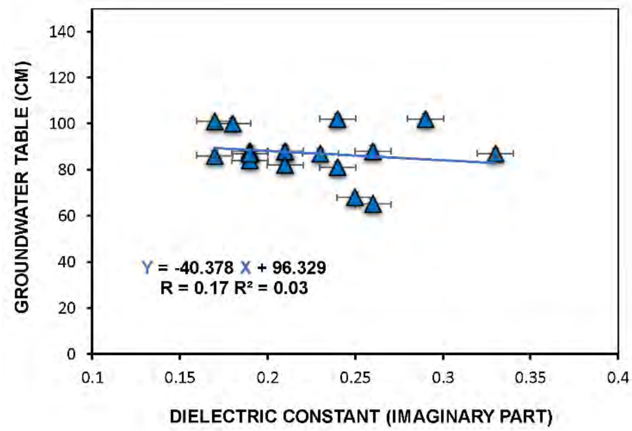


**FIGURE 7.** Relationship graph between dielectric constant (Imaginary part) and groundwater table condition. The relationship is not significant and there is no relationship between the dielectric constant imaginary part and groundwater table.

It means that the relationship is not significant. Relationship graph between the dielectric constant imaginary part and groundwater table is shown in Fig.7.

### *B. BACKSCATTERING COEFFICIENT FROM ALOS-2 PALSAR-2 DATA AND BASED ON IMPEDANCE MODEL SIMULATION*

Backscattering coefficient or Sigma Naught or Sigma 0 from ALOS-2 PALSAR-2 data was calculated by using the equation model by JAXA for ALOS-2 PALSAR-2 data level 1.1. from horizontal-horizontal (HH) Polarization SAR Image. Pixel 5 × 5 was taken to calculate average backscattering coefficient from each point.

Simulation backscattering coefficient based on impedance model was used to generate backscattering coefficient from dry peatland area with groundwater table more than 40 centimeters. Incident angle was calculated based on ALOS-2

**TABLE 3. Incident angle and soil roughness of each sample point position.**

| Point No. | Incidence Angle | Soil Roughness |
|---|---|---|
| 1 | 30.4 | 0.23 |
| 2 | 32.2 | 0.72 |
| 3 | 32.9 | 0.21 |
| 4 | 32.3 | 0.88 |
| 5 | 32.1 | 1.1 |
| 6 | 33.5 | 1.57 |
| 7 | 31.7 | 1.71 |
| 8 | 31.7 | 6.23 |
| 9 | 32.6 | 3.35 |
| 10 | 31.0 | 5.83 |
| 11 | 31.5 | 2.44 |
| 12 | 31.6 | 2.71 |
| 13 | 31.1 | 2.36 |
| 14 | 31.7 | 1.42 |
| 15 | 32.8 | 4.42 |
| 16 | 31.5 | 0.24 |
| 17 | 32.8 | 1.38 |
| 18 | 32.2 | 1.38 |

**TABLE 4. Backscattering coefficient ALOS-2 Data HH polarization and simulation backscattering based on impedance model.**

| Point No. | Backscattering coefficient ALOS-2 data HH Polarization | Simulation Backscattering Based on Impedance Model |
|---|---|---|
| 1 | -12.8 | -12.59 |
| 2 | -13.5 | -11.5 |
| 3 | -12.81 | -12.41 |
| 4 | -12.5 | -14.39 |
| 5 | -13.54 | -14.26 |
| 6 | -16.34 | -17.21 |
| 7 | -14.65 | -14.26 |
| 8 | -13.38 | -14.27 |
| 9 | -12.06 | -12.54 |
| 10 | -13.8 | -13.25 |
| 11 | -12.15 | -14.83 |
| 12 | -11.4 | -11.58 |
| 13 | -13.9 | -12.81 |
| 14 | -13.41 | -13.83 |
| 15 | -14.16 | -15.34 |
| 16 | -16.6 | -17.29 |
| 17 | -15.13 | -15.24 |
| 18 | -13.87 | -13.85 |

PALSAR-2 image and soil roughness was measured from the ground survey, especially point 1 until 5, while soil roughness was calculated based surface elevation model from drone image. Incident angle and soil roughness are shown in Table 3.

Backscattering coefficient from ALOS-2 data HH polarization and simulation backscattering coefficient based on impedance model is shown in Table 4.

Backscattering coefficient from ALOS-2 data image is shown in Table 4. with backscattering coefficient average $-13.67$ dB, minimum $-16.6$ dB, and maximum $-11.4$ dB. Based on the impedance model, backscattering coefficient average $-13.97$ dB, minimum $-11.5$ dB and maximum $-17.29$ dB.

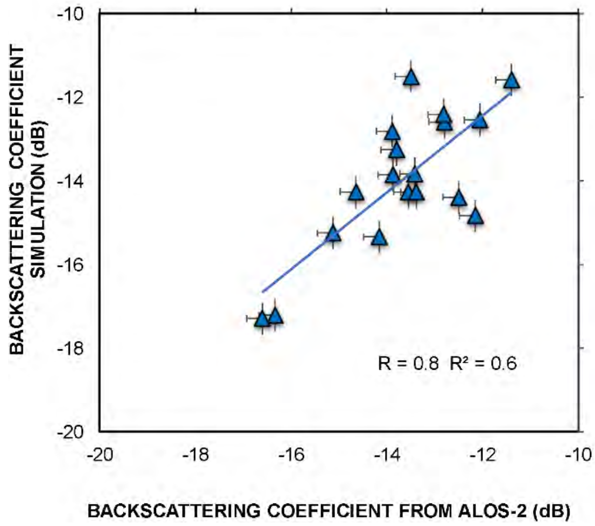


**FIGURE 8.** Relationship graph between simulation backscattering coefficient from impedance model and backscattering coefficient from ALOS-2 PALSAR-2 data. It is shown that the significant correlation (R) is 0.8 and the determinant coefficient ($R^2$) is 0.6.

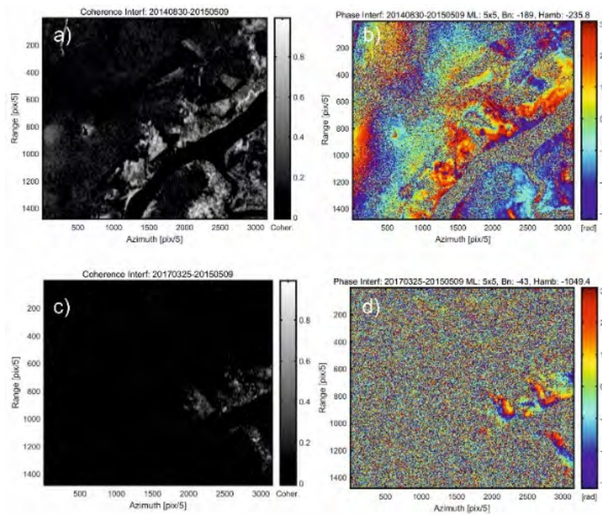


**FIGURE 9.** (a) Coherence map and (b) Interferogram of DInSAR analysis using ALOS-2 PALSAR-2 data for images acquired on August 30 2014 and 9 May 2015, and (c) Coherence Map and (d) Interferogram of DInSAR analysis using ALOS-2/PALSAR-2 data for images acquired on 2017 March 25 and May 9, 2015.

### *C. CORRELATION BACKSCATTERING COEFFICIENT ALOS-2 DATA AND SIMULATION BACKSCATTERING COEFFICIENT BASED ON IMPEDANCE MODEL*

In this research, the correlation between backscattering from ALOS-2 PALSAR-2 horizontal-horizontal polarization data and simulation backscattering based on impedance model was calculated. Mac Pearson's correlation coefficient was applied to this model. Furthermore, based on calculation, the correlation between simulation backscattering by using impedance model and simulation from ALOS-2 data is significant, 0.8, and the coefficient determinant is 0.6, and RMSE is 1.4, shown in Fig.8. It means that by using ALOS-2 data, detection of peatland risk fire area was successful. Backscattering coefficient from ALOS is representative of

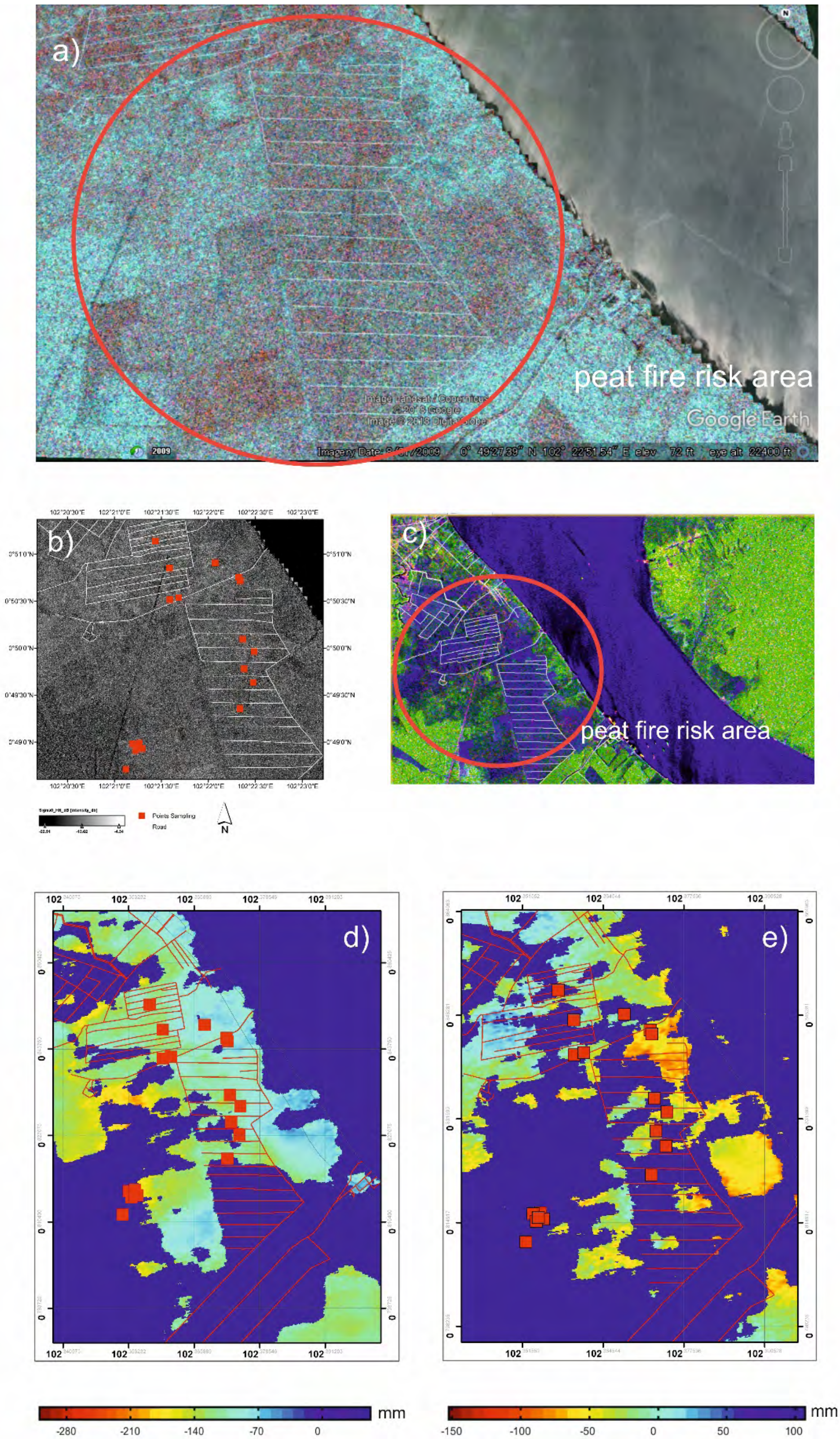


**FIGURE 10.** **a) Peat fire risk area shown in red color based on detection by using an impedance model approach (b) Backscattering coefficient map HH polarization ALOS-S PALSAR-2 data (c) Peat fire risk area on RGB composit of Yamaguchi Decomposition with R is double helix scattering, G is volume scattering, and B is surface scattering (d) Subsidence condition in reserach area based on DInSAR approach for pair Images A, and (e) Subsidence condition in reserach area based on DInSAR approach for pair images B.**

dry peat area with small dielectric constant value. The area with dry peat and deep groundwater table then is associated with peat fire risk area.

### D. DInSAR APPROACH

This research was also proposed to detect peat fire risk area by using DInSAR Approach. In this research, DInSAR approach was used to support a thesis based on the result of the impedance model approach. DInSAR approach was used under the assumption that there is a significant relationship between subsidence and groundwater table [32].

By using DInSAR, 2 pairs of ALOS-2 data acquired on August 2014, May 2015, and March 2017 were processed. ALOS-2 PALSAR-2 data in Single Look Complex (SLC) was used as master and slave image to coregistration process. Pair A used image of ALOS-2 PALSAR-2 acquired on May 9, 2015 as master and image acquired on August 30, 2014 as a slave. Pair B used image acquired on May 9, 2015 as master and image acquired on March 25, 2017 as a slave. After coregistration, phase interferogram developed. Thus, coherence map and phase interferogram are shown in Fig. 9

For DInSAR approach of Pair A, phase interferogram developed with Multi Looking 5 × 5 pixels, Goldstein Filtering 5 × 5 pixels, and Normal Baseline 189 m, and ambiguity 235.8. Pair B, phase interferogram developed with Multi Looking 5 × 5 pixels, Goldstein Filtering 5 × 5 pixels, and Normal Baseline −43 m, and ambiguity 1049.4. The short normal baseline can guarantee the quality of interferogram [20].

From coherence map, it can be denoted that the coherence map of Pair A is wider then Pair B. Based on DInSAR process of pair A and Pair B, there is a condition that not all 18 points used on an impedance model simulation are coherent on DInSAR approach. Based on Pair A, there are 10 points of coherence and based on Pair B, there are 7 points of coherence. The time range was also different between Pair A and Pair B; Pair A is 9 months and Pair B is 24 months. Due to this condition, for calculation of annual subsidence rate, correction factor was used for Pair A and Pair B.

The result subsidence of Pair A was then multiplied by 12/9 to calculate the annual subsidence rate, and the result of subsidence of Pair B divided by 2 to calculate the annual subsidence rate. Annual subsidence rate of Pair A average was 6.6 cm/year, with a minimum of 6 cm/year, and a maximum 7.5 cm/year. Annual subsidence rate for Pair B average was 2.8 cm/year, minimum 2,5 cm/year, and maximum 3.5 cm/year. The range of time for Pair A is related to El Nino in Indonesia, when the condition is very dry and many forest fire occurs in Indonesia [5].

By using Woosten Model [29], the relationship between annual rate subsidence and groundwater table depth was explained. Groundwater table based on DInSAR aproach then is calculated and shown in Table 5.

Based on Table 5, the simulation groundwater table for Pair A in average is 165.6 cm, with minimum value 150 cm and maximum 187 cm. Simulation groundwater table for Pair B in average is 69.4 cm, with minimum value 63 cm and maximum value 87 cm.

Based on the simulation of groundwater table, it shows that the groundwater table for each point is lower than 40 cm and indicated that the peatland area is very risky to fire. During the field survey peat fire also happened in the field area, and helicopter used water boom to protect the fire.

Correlation between the simulation of groundwater table and groundwater table based on the field survey then compare by using Mac Pearson's correlation test for validation. Based on a correlation test between simulation groundwater table of Pair A and field survey gave a correlation coefficient (R) value 0.71, and determination coefficient ($R^2$) 0.51. Then, correlation test between simulation table of Pair B and field survey gave correlation value (R) 0.85 and determination coefficient ($R^2$) 0.73. Graph of the test shown in Fig. 11

**TABLE 5. Annual subsidence rate and simulation of groundwater table based on DInSAR approach.**

| Point No. | Annual Subsidence Rate (cm/year) | | GWT Depth Simulation (cm) | |
|---|---|---|---|---|
| | Pair A | Pair B | Pair A | Pair B |
| 1 | 6.7 | - | 167 | - |
| 2 | 6 | 2.5 | 150 | 63 |
| 3 | - | 3.2 | - | 80 |
| 4 | 6.4 | 3.2 | 167 | 79 |
| 5 | 6.4 | - | 167 | - |
| 6 | 7.5 | - | 187 | - |
| 7 | - | - | - | - |
| 8 | - | - | - | - |
| 9 | 6.4 | 3.3 | 160 | 82 |
| 10 | 6.4 | 3.5 | 160 | 87 |
| 11 | - | - | - | - |
| 12 | - | - | - | - |
| 13 | - | - | - | - |
| 14 | - | - | - | - |
| 15 | - | - | - | - |
| 16 | 6.7 | 3.4 | 167 | 84 |
| 17 | 6.7 | - | 167 | - |
| 18 | 6.7 | 3.3 | 167 | 81 |

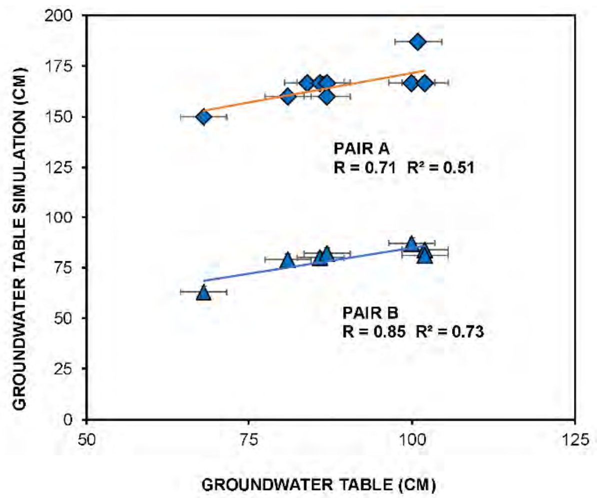


**FIGURE 11. The relationship between simulation groundwater table of Pair A (red line) and Pair B (blue line) DInSAR approach and groundwater table based on field survey and meassurement.**

From DInSAR approach, it is shown that this method is also possible to detect peat fire risk area.

## V. CONCLUSION

From this research, detection of peat fire risk area was successfully carried out by using three layer of new impedance model approach that addition of soil roughness parameter as a layer between air and soil surface and as apart of novelty of this research. Peat fire risk area was denoted as backscattering value between −11.5 until −17,29 dB in HH Polarization ALOS-2 PALSAR-2 data. Correlation between simulation of backscattering coefficient and backscattering coefficient from ALOS-2 data measurement gave high correlation, 0.8. Based on the result, DInSAR approach also successfully detected fire risk area following the groundwater table simulation. The location with groundwater table more than 40 cm is associated with peat fire risk area. The correlation test also gave significant result 0.71 for Pair A and 0.85 for Pair B. Both impedance model and DInSAR approaches gave the significant result to detect peat fire risk area and was indicated based on high correlation coefficient. The combination of the new impedance model method and DInSAR approaches as other innovations of this research is shown to provide advantage in the form of accurate analysis results because of cross-checking in each other.

## ACKNOWLEDGMENT

The authors would like to thank Siak Regency Local Government, and Universitas Islam Riau, Republic of Indonesia.

## REFERENCES

[1] M. Osaki, D. Nursyamsi, M. Noor, and S. H. Wahyunto, "Peatland in Indonesia," in *Tropical Peatland Ecosystems*, vol. 1, 1st ed. Tokyo, Japan: Springer, 2016, pp. 49–57.

[2] S. N. Qodriyatun, "KebijakanPenangananKebakaranHutan dan Lahan," *InfoSingkatKesejahteraanSosial, Pusat PengkajianPengolahan Data Informasi*, DPR-RI, vol. 6, no. 6/II/P3DI, pp. 1–4, Mar. 2014.

[3] P. Hirschberger, "Forests ablaze: Causes and effects of global forest fires," WWF, Berlin, Germany, 2017.

[4] World Bank, Washington, DC, USA. (2016). *The Cost of Fire: An Economic Analysis of Indonesia's 2015 Fire Crisis (English)*. Indonesia Sustainable Landscapes Knowledge; Note No. 1. [Online]. Available: http://documents.worldbank.org/curated/en/776101467990969768/The-cost-of-fire-an-economic-analysis-of-Indonesia-s-2015-fire-crisis

[5] W. J. de Groot, R. D. Field, M. A. Brady, O. Roswintiarti, and M. Mohamad, "Development of the Indonesian and Malaysian fire danger rating systems," *Mitigation Adaptation Strategies Global Change*, vol. 12, pp. 165–180, Jan. 2006.

[6] G. Caccamo, L. A. Chisholm, R. A. Bradstock, and M. L. Puotinen, "Using remotely-sensed fuel connectivity patterns as a tool for fire danger monitoring," *Geophys. Res. Lett.*, vol. 39, p. L01302, Jan. 2012. doi: 10.1029/2011GL050125.

[7] E. H. Chowdhury and Q. K. Hassan, "Operational perspective of remote sensing-based forest fire danger forecasting systems," *ISPRS J. Photogramm. Remote Sens.*, vol. 104, pp. 224–236, Jun. 2015. doi: 10.1016/J.isprsjprs.2014.03.011

[8] B. Leblon, "Monitoring forest fire danger with remote sensing," *Natural Hazards*, vol. 35, no. 3, pp. 343–359, 2005. doi: 10.1007/S11069-004-1796-3.

[9] H. Sunuprapto and Y. A. Hussin, "A comparison between optical and radar satellite images in detecting burnt tropical forest in South Sumatra, Indonesia," *Int. Arch. Photogramm. Remote Sens.*, vol. 33, pp. 580–587, 2000.

[10] K. N. Abbott, B. Leblon, G. C. Staples, D. A. Maclean, and M. E. Alexander, "Fire danger monitoring using RADARSAT-1 over northern boreal forests," *Int. J. Remote Sens.*, vol. 28, no. 6, pp. 1317–1338, 2007. doi: 10.1080/01431160600904956.

[11] L. L. Bourgeau-Chavez, E. S. Kasischke, and M. D. Rutherford, "Evaluation of ERS SAR data for prediction of fire danger in a boreal region," *Int. J. Wildland Fire*, vol. 9, no. 3, pp. 183–194, 1999. doi: 10.1071/.WF00009.

[12] L. L. Bourgeau-Chavez *et al.*, " Remote monitoring of spatial and temporal surface soil moisture in fire disturbed boreal forest ecosystems with ERS SAR imagery," *Int. J. Remote Sens.*, vol. 28, no. 10, pp. 2133–2162, 2007. doi: 10.1080/01431160600976061.

[13] M. A. Tanase, R. Panciera, K. Lowell, and C. Aponte, "Monitoring live fuel moisture in semiarid environments using L-band radar data," *Int. J. Wildland Fire*, vol. 24, no. 4, pp. 560–572, 2015.

[14] Y. Izumi *et al.*, "Potential of soil moisture retrieval for tropical peatlands in Indonesia using ALOS-2 L-band full-polarimetric SAR data," *Int. J. Remote Sens.*, to be published.

[15] K. Hirose *et al.*, "Contribution of hyperspectral applications to tropical peatland ecosystem monitoring," in *Tropical Peatland Ecosystems*, vol. 1, 1st ed. Tokyo, Japan: Springer, 2016, pp. 421–430.

[16] J. Widodo, Y. Izumi, A. Takahashi, H. Kausarian, H. Kuze, and J. T. S. Sumantyo, "Detection of dry-flammable peatland area by using backscattering coefficient information of ALOS-2 data L-band frequency," in *Proc. Prog. Electromagn. Res. Symp. (PIERS-Toyama)*, Toyama, Japan, 2018, pp. 916–920. doi: 10.23919/PIERS.2018.8598099.

[17] A. P. Dimitrakopoulos and K. K. Papaioannou, "Flammability assessment of Mediterranean forest fuels," *Fire Technol.*, vol. 37, pp. 143–152, Apr. 2001. doi: 10.1023/A:1011641601076.

[18] (Sep. 15, 2014). *Peraturan Pemerintah No. 71, 2014, Perlindungan dan Pengelolaan Ekosistem Gambut*. Accessed: Mar. 5, 2018. [Online]. Available: http://peraturan.go.id/pp/nomor-71-tahun-2014-11e4a07c7288d63ab190313531353038.html

[19] (2016). *Peraturan Pemerintah No. 57, 2016, Perubahan Atas Peraturan Pemerintah No. 71 Tahun 2014 Tentang Perlindungan dan Pengelolaan Ekosistem Gambut*. Accessed: May 14, 2018. [Online]. Available: http://peraturan.go.id/pp/nomor-57-tahun-2016.html

[20] P. Mishra, S. Goel, and D. Singh, "An impedance based approach to determine soil moisture using radarsat-2 data," in *Proc. IGARSS*, Melbourne, VIC, Australia, 2013, pp. 2724–2727.

[21] S. S. J. Tetuko, R. Tateishi, and N. Takeuchi, "Estimation of burnt coal seam thickness in central Borneo using JERS-1 SAR data," *Int. J. Remote Sens.*, vol. 24, no. 4, pp. 879–884, 2003.

[22] S. S. J. Tetuko, R. Tateishi, and N. Takeuchi, "A physical method to analyze scattered wave from burnt seam and its application to estimate thickness of fire scars in central Borneo using L-Band SAR data," *Int. J. Remote Sens.*, vol. 24, no. 15, pp. 3119–3136, 2003.

[23] H. Al-Bilbisi, R. Tateishi, and S. S. J. Tetuko, "A technique to estimate topsoil thickness in arid and semi-arid areas of north-eastern Jordan using synthetic aperture radar data," *Can. J. Remote Sens.*, vol. 43, no. 2, pp. 95–108, 2017.

[24] H. Kausarian, S. S. J. Tetuko, H. Kuze, J. Aminuddin, and M. M. A. Waqar, "Analysis of polarimetric decomposition, backscattering coefficient, and sample properties for identification and layer thickness estimation of silica sand distribution using L-band synthetic aperture radar," *Adv. Remote Sens.*, vol. 4, no. 2, pp. 15–24, 2015. doi: 10.1080/07038992.2017.1286935.

[25] D. Perissin, "Interferometric SAR multitemporal processing: Techniques and applications," in *Multitemporal Remote Sensing*. Cham, Switzerland: Springer, 2016, pp. 145–176.

[26] Z. Zhou, "The applications of InSAR time series analysis for monitoring long-term surface change in peatlands," Ph.D. dissertation, School Geographi. Earth Sci., Univ. Glasgow, Scotland, U.K., Sep. 2013.

[27] Z. Zhou, Z. Li, A. Tanaka, and S. Waldron, "Monitoring peat subsidence and carbon emission in Indonesia peatlands using InSAR time series," in *Proc. IGARSS*, Beijing, China, 2016, pp. 6797–6798.

[28] W. Takeuchi, T. Hirano, and O. Roswintiarti, "Estimation model of ground water table at peatland in central Kalimantan, Indonesia," in *Tropical Peatland Ecosystems*, vol. 1, 1st ed. Tokyo, Japan: Springer, 2016, pp. 445–453.

[29] J. H. M. Wösten, A. B. Ismail, and A. L. M. van Wijk, "Peat Subsidence and its practical implications: A case study in Malaysia," *Geoderma*, vol. 78, pp. 25–36, Jul. 1997.

[30] *BPS Siak, Siak Dalam Angka 2016, Siak Regency, Indonesia 2016*. Accessed: Jul. 1, 2018. [Online]. Available: https://siakkab.bps.go.id/publication/2017/08/11/1b653bc3cb27d9fb06ed7fbc/kabupaten-siak-dalam-angka-2017.html

[31] A. D. Subekty and S. G. Neuzil, "General geology and peat resources of the Siak Kanan and Bengkalis Island peat deposits, Sumatra, Indonesia," Geological Soc. Amer., Special Paper 286, 1993, pp. 45–62. doi: 10.1130/SPE286-p45.

[32] O. Isoguchi, M. Sakashita, and M. Shimada. ALOS-2 PALSAR-2 Cal/Val Updates, Joint PI Meeting of Global Environment Observation Mission FY 2017. Tokyo, Japan. Accessed: Jul. 2018. [Online]. Available: http://www.eorc.jaxa.jp/ALOS-2/en/calval/JAXA_PI_workshop_ALOS2CalVal_20180124.pdf

[33] Y. Li, K. Zhao, J. Ren, Y. Ding, and L. Wu, "Analysis of the dielectric constant of saline-alkali soils and the effect on radar coefficient: A case study of soda alkaline saline soils in western Jilin province using RADARSAT-2 data," *Sci. World J.*, vol. 2014, pp. 1–14, 2014. doi: 10.1155/2014/563015.

[34] G. E. Susilo, K. Yamamoto, and T. Imai, "Modeling groundwater level fluctuation in the tropical peatland areas under the effect of El Nino," *Procedia Environ. Sci.*, vol. 17, pp. 119–128, 2013.

[35] J. H. M. Wösten, E. Clymans, S. E. Page, J. O. Rieley, and S. H. Limin, "Peat–water interrelationships in a tropical peatland ecosystem in Southeast Asia," *Catena* vol. 73, no. 2, pp. 212–224, Apr. 2008.

[36] J. O. Rieley, S. E. Page, and J. Jauhiainen, *Wise Use of Tropical Peatlands: Focus on Southeast Asia: Synthesis of Results and Conclusions of the UK Darwin Initiative and the EU INCO EUTROP, STRAPEAT AND RESTORPEAT Partnerships Together With Proposals for Implementing Wise Use of Tropical Peatlands*. Wageningen, The Netherlands: Alterra, 2005.

[37] H. Takahashi, A. Usup, H. Hayasaka, and S. H. Limin, "Estimation of ground water levels in a peat swamp forest as an index of peat/forest fire," in *Proc. Int. Symp. Land Manage. Biodiversity Southeast Asia*. Bali, Indonesia, Sep. 2002, pp. 17–20.

[38] A. Usup, Y. Hashimoto, H. Takahashi, and H. Hayasaka, "Combustion and thermal characteristics of peat fire in tropical peatland in Central Kalimantan, Indonesia," *Tropics*, vol. 14, no. 1, p. 119, 2004.

[39] E. S. Adiningsih, "Monitoring El Nino and La Nina phenomenon: The use of remote sensing for land forest fire anticipation," *Warta LAPAN*, vol. 3, no. 2, pp. 45–55, 2001.

**JOKO WIDODO** (M'01) was born in Yogyakarta, Indonesia. He received the B.S. degree in geography from Gadjah Mada University, in 1999, and the M.S. degree in environmental science from the University of Indonesia, in 2012. He is currently pursuing the Ph.D. degree with the Graduate School of Advance and Integration Science, Chiba University, Japan. From 1999 to 2005, he was a Consultant of GIS and remote sensing in Indonesia. Since 2005, he has been an Engineer with the Agency for the Assessment and Application of Technology, Indonesia. His research and work focus on environmental assessment, GIS, and remote sensing. His research interests include polarimetric synthetic aperture radar, interferometry synthetic aperture radar, and permanent scattered synthetic aperture radar.

**YUTA IZUMI** received the B.Eng. degree from the Center for Environmental Remote Sensing (CEReS), Graduate School of Advanced Integration Science, Chiba University, Japan, in 2016, and the M.Eng. degree from the Josaphat Microwave Remote Sensing Laboratory, CEReS, Chiba University, in 2018. He is currently pursuing the Ph.D. degree with the Graduate School of Environmental Studies, Tohoku University, Japan. His research interests include polarimetric radar calibration, soil moisture retrieval, atmospheric phase screen compensation for GB-SAR, and polarimetric interferometric analysis for GB-SAR. He was a recipient of the President Award of Chiba University and the Dean Award of the Graduate School of Advanced Integration Science, Chiba University, in 2018.

**AYAKA TAKAHASHI** was born in Chiba, Japan. She received the B.S., master's, and Ph.D. degrees in aerospace engineering and space tribology from Teikyo University, Japan. She was a member of the High Temperature Material Laboratory. She is currently a Research Staff with Chiba University. Her research topic is about antenna material for synthetic aperture radar and solid lubricant for driving system of space craft.

**HUSNUL KAUSARIAN** was born in Dumai, Indonesia, in 1986. He received the B.S. degree in geology and the M.S. degree in geological engineering from the National University of Malaysia, in 2007 and 2009, respectively, and the Ph.D. degree in remote sensing geology from Chiba University, Japan, in 2017.

In 2011, he joined the Geological Engineering Department, Universitas Islam Riau, as an Assistant Professor, where he became a Senior Lecturer, in 2016. He has been actively doing research, since 2009. His research interests include geological mapping using conventional and remote sensing approach for natural resource, oil and gas, mineral distribution, urban design, power plant design, and mitigation. He was a recipient of the Dean Award as the Best Student during his Ph.D. research, in 2017, and the International Award for Himalaya Geological Expedition, in 2017.

**DANIELE PERISSIN** was born in Milan, Italy, in 1977. He received the master's degree in telecommunications engineering and the Ph.D. degree *(cum laude)* in information technology from the Politecnico di Milano, in 2002 and 2006, respectively. In 2002, he was involved in the permanent scatters technique in the framework of microwave remote using synthetic aperture radar. After 2009, he joined the Institute of Space and Earth Information Science, The Chinese University of Hong Kong. He is a Developer of Sarproz Software, specialist software for interferometric synthetic aperture radar and permanent scatters synthetic aperture radar. He has authored more than 90 paper journals.

**JOSAPHAT TETUKO SRI SUMANTYO** (SM'12) was born in Bandung, Indonesia, in 1970. He received the B.Eng. and M.Eng. degrees in electrical and computer engineering (subsurface radar systems) from Kanazawa University and the Ph.D. degree in artificial system sciences, in 2002. Between 2002 and 2005, he was a Lecturer with the Center for Frontier Electronics and Photonic (Postdoctoral Fellowship Researcher) and continued as an Associate Professor with the Center for Environmental Remote Sensing, Chiba University, Japan. Since 2013, he has been a Full Professor (permanent staff) with Chiba University. He is also as a Visiting Lecturer with many universities. He founded and manages Josaphat Microwave Remote Sensing Laboratory, Center for Environmental Remote Sensing, Chiba University, Japan. His researches focus on synthetic aperture radar, especially circular polarized synthetic aperture radar, polarimetric SAR, InSAR, and PS-InSAR. He received many awards and research grants related to his researches and studies. He has promoted many students from around the world.